Applied Catalysis B: Environmental 99 (2010) 298–306

Contents lists available at ScienceDirect

Applied Catalysis B: Environmental

journal homepage: www.elsevier.com/locate/apcatb

Catalyst studies on the hydrotreatment of fast pyrolysis oil

J. Wildschut, I. Melián-Cabrera, H.J. Heeres*

Department of Chemical Engineering, Institute of Technology and Management, University of Groningen, Nijenborgh 4, 9747 AG, Groningen, The Netherlands

ARTICLE INFO

Article history:
Received 26 February 2010
Received in revised form 21 June 2010
Accepted 23 June 2010
Available online 30 June 2010

Keywords:
Fast pyrolysis oil
Upgrading
Catalytic hydrotreatment
Ruthenium on carbon
Catalyst deactivation

ABSTRACT

Catalytic hydrotreatment is considered an attractive technology for fast pyrolysis oil upgrading to liquid transportation fuels. We here report an experimental study to gain insights in catalyst stability when using Ru/C catalysts for the hydrotreatment of fast pyrolysis oil (350 °C and 200 bar) in a batch reactor set-up. A considerable reduction in the liquid yield (55–30 wt.%), increased solids formation (3–20 wt.%), a reduction in the H/C ratio (1.24–1.08) of the liquid product and a lowering of the extent of methane in the gas phase was observed after a number of catalyst recycles. Characterization of the catalyst before and after reaction using TEM, chemo- and physisorption showed significant coke deposition and a decrease in pore volume and metal dispersion. The application of in-house prepared Ru/C catalysts for both the hydrotreatment of fast pyrolysis oil as well as phenol using different Ru-precursors ($RuCl_3$, $Ru(NO)(NO_3)_3$ and $Ru(acac)_3$) gave different results for the various catalysts with respect to product yield (45–56 wt.% for fast pyrolysis oil) and elemental composition of the liquid phase. A catalyst prepared from the precursor $RuCl_3$ at a ruthenium loading of 5 wt.% showed the highest activity for the hydrogenation reaction of fast pyrolysis oil (H/C of 1.32 vs. 1.24 for the commercial Ru/C catalyst) and the lowest reduction in BET area and metal dispersion after reaction.

1. Introduction

Liquid transportation fuels from biomass sources are considered attractive alternatives for the current fossil-derived fuels. A variety of technologies have been investigated for the conversion of biomass into liquid transportation fuels. Well-known examples are biodiesel from plant oils and bioethanol from carbohydrate rich resources [1]. Due to competition with the food industry, these first generation biofuels are under pressure and new options are being explored actively [1]. A promising second generation biofuel platform involves thermochemical biomass conversions like gasification, hydrothermal liquefaction and fast pyrolysis [1]. Fast pyrolysis technology involves the rapid heating of lignocellulosic biomass to temperatures in the range of 450–650 °C with a residence time of <2 s in an oxygen-free atmosphere [2]. Typical liquid product yields for this technology are up to 70 wt.% [2]. The resulting oil is a multi-component mixture that contains up to several hundreds of components with a wide variety of functional groups and molecular weights. Typical compound classes are organic acids, aldehydes, ketones, phenolics and alcohols. The resulting oil as such is not suitable as a biofuel for high-speed internal combustion engines. The oil contains large amounts of water (up to 30 wt.%, higher amounts result in phase separation) and corrosive organic acids (up to 10 wt.%) [2,3] and shows limited storage stability. Upgrading by either chemical or physical methods is required [2].

Catalytic hydrotreatment is considered a promising upgrading technology [4]. This process involves treatment of fast pyrolysis oil with hydrogen in the presence of a heterogeneous catalyst. The primary aim is a reduction/minimization of the oxygen content by hydrodeoxygenation (HDO), leading to gasoline or diesel like products. Research activities on the HDO of pyrolysis oil started already in 1984 with the pioneering work of Elliott and Baker [4]. Typically, batch or trickle bed reactors (packed beds with downflow operation of both liquid and gas) in continuous mode were applied in combination with commercial HDS catalysts, i.e. sulphided $NiMo/Al_2O_3$ and $CoMo/Al_2O_3$ [4–9].

One of the disadvantages of the latter two catalysts is the requirement of the presence of sulphur to remain active. Furthermore, deactivation of the catalysts as a function of time on stream is reported. Different deactivation mechanisms have been proposed like blockage of catalyst pores and active sites, poisoning of the catalyst (by, for example, nitrogen compounds), sintering of the active metals, structural degradation of the support and active sites, coking and metal deposition [9]. The main cause for catalyst deactivation appears coke formation, which may result in blockage of the catalyst pores and thus limiting the access of reactants into the pores [3,10–13]. The tendency for coking is a function of the chemical structure and activity of the catalyst support. The coking rate is lower using neutral carriers whereas commonly used alumina supports are known to promote coke formation [14]. Model

* Corresponding author. Tel.: +31 50 363 4174; fax: +31 50 363 4479.
E-mail address: h.j.heeres@rug.nl (H.J. Heeres).

0926-3373/$ – see front matter © 2010 Elsevier B.V. All rights reserved.
doi:10.1016/j.apcatb.2010.06.036

compound studies suggest that phenolic components are mainly responsible for coke formation, though there are also indications that the carbohydrate fraction in fast pyrolysis oil is responsible for coke formation [5,15–17].

To improve the economic incentive, improved catalysts for the hydrotreatment of pyrolysis oil are highly desirable. These should be active and stable, produce high liquid yields and not result in the formation of (large amounts of) coke. Noble metal catalysts based on Ru, Pd, Rh, Pt as well others metals like CuCr, CuO, NiO and Ni on various supports have been explored [4–8,10,18–23]. Recently we reported a catalyst screening study in a batch set-up at well-defined conditions with a range of noble metal catalysts (Ru/C, Ru/TiO_2, Ru/Al_2O_3, Pt/C and Pd/C) at 250–350 °C and 100–200 bar pressure. Good performance of the Ru/C catalyst with respect to oil yield (up to 60 wt.%) and deoxygenation level (up to 90 wt.%) was observed [24]. In a subsequent study the Ru/C catalyst was explored in more detail and the effect of reaction times on oil yield and product properties was determined [25]. In autoclave experiments at 350 °C and 200 bar, a 4 h reaction time appears to be optimal with respect to oil yield. Longer reaction times lead to a reduction of the oil yield due to gasification. Solids formation (coke) was observed for all experiments, the highest amounts being 5.3 wt.%.

Studies aimed at determining the stability of Ru/C catalysts for the hydrotreatment of fast pyrolysis oils are limited. We here report experiments to determine the level of catalyst deactivation when using Ru/C catalysts for the hydrotreatment of fast pyrolysis oil. Furthermore, the effect of the type of catalyst precursor for the synthesis of the Ru/C catalyst ($Ru(NO)(NO_3)_3$, $RuCl_3$ and $Ru(acac)_3$) on catalytic activity and stability was explored for hydrotreatment experiments with fast pyrolysis oil as well as for model studies with phenol. The performance of Ru/C catalysts is known to be affected by the metal precursors used in the preparation step [26,27]. For instance, Miyazawa et al. used various Ru/C catalyst in combination with an Amberlyst ion-exchange resin for the dehydration and hydrogenation of glycerol to 1,2-propanediol at mild reaction conditions (120 °C) [26]. Catalyst activity and product selectivity were a strong function of the ruthenium precursor ($RuCl_3$, $Ru(NO)(NO_3)_3$ or $Ru(acac)_3$) used for the preparation of the Ru/C catalyst. Similar observations were made by Neri et al. for the hydrogenation of citral (60 °C in ethanol) using various ruthenium-based catalysts [27]. In the present work, relevant catalyst properties (dispersion, BET surface areas and the size of the ruthenium metal clusters) were measured and critically evaluated before and after reaction to probe possible catalyst deactivation mechanisms.

2. Materials and methods

2.1. Materials

$Ru(NO)(NO_3)_3$ (1.5 wt.% solution in water), $Ru(acac)_3$ (99%, acac = acetylacetonate) and $RuCl_3$ anhydrous (99%) were obtained from Strem chemicals. Activated carbon (SG Ultra, 1200 m^2/g) with an average particle size of 17.3 ± 4.5 μm was used as the carrier and supplied by Norit (The Netherlands). Phenol was obtained from Sigma–Aldrich. Fast pyrolysis oil was supplied by BTG (Enschede, The Netherlands) and was derived from beech wood (Table 1) and was used as received. The commercial Ru/C catalyst (5 wt.% of active metal) was obtained from Sigma–Aldrich. The average particle diameter was 18.4 ± 4.8 μm. Hydrogen, nitrogen and helium were obtained from Hoekloos (Schiedam, The Netherlands) and were all of analytical grade (>99.9999%). Tetrahydrofuran (THF), *n*-decane and dodecane were obtained from Acros (99.99%).

Table 1
Properties of the fast pyrolysis oil used in this study.

Property	Value
Water content (wt.%)	25
Elemental composition, dry base (wt.%)	
C	55.4
H	6.9
O	37.7

2.2. Catalyst preparation

All catalysts were prepared by wet impregnation. In case of $Ru(acac)_3$, acetone was used as a solvent, whereas water was used for the other two precursors. The synthesis was performed by suspending 10 g of active carbon in a solvent (water or acetone, 100–200 ml). Subsequently, a pre-determined amount of the metal precursor was added to obtain the preferred Ru amount on carrier (1, 3 or 5 wt.%). The suspension was stirred for 24 h under air (20 °C and 1 bar). After stirring, the solvent was evaporated at reduced pressure (35–40 °C, ~30 mbar) for 8 h. Then the catalyst was dried at 100 °C for 12 h under vacuum (35 mbar). After drying, the catalysts were treated at 250 °C for 2 h in a nitrogen atmosphere. During this procedure, the nitrogen atmosphere was refreshed six times. The catalyst was stored under a protective nitrogen atmosphere.

2.3. Experimental set-ups

Fast pyrolysis oil was hydrotreated in a 100 ml batch autoclave set-up (Buchi AG, CH Uster, max. 350 bar, 450 °C). Phenol was hydrotreated in a 100 ml Parr autoclave (max. 350 bar, 350 °C). The reactors were equipped with an electric heater and cooling coil (water) to allow operation at constant temperature. The reaction mixture was stirred with a magnetically driven gas inducing impeller at 1300 rpm of the Ruston type (*d*: 24 mm, h: 12 mm and 5 mm thickness). Temperature and pressure were continuously measured in the reactor vessel and monitored by a computer.

2.3.1. Fast pyrolysis oil hydrotreatment experiments

For a typical experiment, the reactor was filled with fast pyrolysis oil (25 g) and catalyst (1.25 g, 5 wt.% with respect to pyrolysis oil), and subsequently flushed with nitrogen gas and then pressurized with 20 bar of hydrogen gas at room temperature. The reactor was heated to the intended reaction temperature (350 °C) with a heating rate of 16 °C/min. The pressure in the reactor was increased to 200 bar by adding hydrogen. After 4 h reaction time at 350 °C (4.3 h time when including heating up period to 350 °C), the reactor was cooled to ambient temperature, the pressure recorded for mass balance calculations and the gas phase was sampled using a gas bag. The liquid phase (consisting of an aqueous and one or two oil phases) was recovered from the reactor using a syringe and weighed. The solids were collected, washed with acetone, dried and weighed till constant weight. The weight of the solids was corrected for the catalyst intake.

In the recycling experiments, the solids were isolated from the liquid (oil and aqueous phase). These were mixed with a 10-fold excess of acetone. Subsequently the mixture was filtered and the solid residue was washed three times with acetone to remove the carbon deposit. The solids were dried 24 h (100 °C and 30 mbar) and reused for a subsequent hydrotreatment reaction without a pre-activation step.

2.3.2. Catalytic hydrotreatment experiments with phenol

The Ru/C catalysts were activated prior to reaction. For this purpose, the reactor was loaded with the catalyst, charged with hydrogen gas (5–10 bar) at room temperature and then heated to 250 °C. After activation for 2 h, the reactor was cooled to room temperature and filled with 5 g of phenol, 20 g of dodecane and the

Ru/C catalyst. Subsequently, the reactor was flushed with nitrogen gas to remove all oxygen and then filled with hydrogen gas at room temperature (10 bar). The reactor was heated to the reaction temperature (250 °C) with a heating rate of about 20 °C/min. The hydrogen pressure was increased to the pre-determined value (100 bar) when the reaction temperature was reached. During reaction, the reactor content was stirred at 1300 rpm. Liquid samples were taken every 10 min during the first hour. After 1 h, samples were taken every hour. The liquid samples were analyzed with GC–MS, 2D-GC and GC–TCD. A typical reaction time was 4.3 h.

2.4. Analysis of the various liquid phases

For all GC analyses (GC–MS, 2D-GC), the samples were injected either pure or diluted (50 wt.%) with THF. Phenol and phenol hydrotreatment product samples were dissolved in THF and *n*-decane was used as an internal standard. Details about equipment and analytical procedures for GC–MS and 2D-GC measurements are given in reference [24].

Elemental analysis (C, H and N) were determined using an Euro Vector 3400 CHN-S analyzer. The oxygen content was determined by difference.

The water content in the samples was determined by Karl Fischer titration using an Metrohm Titrino 758 titration device. A small amount of sample (ca. 0.03-0.05 g) was added into an isolated glass chamber containing Hydranal® (Karl Fischer Solvent, Riedel de Haen). The titrations were carried out using the Karl Fischer titrant Composit 5K (Riedel de Haen). All measurements were performed in duplicate.

2.5. Gas phase analysis

Details about equipment and analytical procedures for gas phase analyses are given in reference [24].

2.6. Catalyst characterization

Monolayer hydrogen chemisorption capacity and dispersion measurements were performed with a Coulter Omnisorp 100C× gas adsorption instrument using static volumetric adsorption method. Before a measurement the sample was evacuated at room temperature to a pressure of 2.67×10^{-8} bar or lower, heated in vacuum to 150 °C and purged in helium flow for 30 min. After this drying treatment, the sample was reduced in a hydrogen flow at 400 °C for 1 h and then evacuated at the same temperature for 1 h. In all steps, a temperature ramp of 10 °C/min and a gas flow rate of 35 cm^3/min were applied. The total hydrogen adsorption isotherm was measured at room temperature up to 0.33 bar by dosing hydrogen to the sample and measuring the adsorbed amount as a function of hydrogen pressure. After adsorption, the sample was evacuated at the same temperature for 1 h and the adsorption measurement was repeated for reversible adsorption. Finally, after the chemisorption measurement, a dead space calibration with helium was performed.

The measured adsorption isotherms were used to calculate the monolayer surface capacity. A linear regression was applied to both isotherms individually for the linear region of the curve, typically between 0.07 and 0.27 bar. Extrapolation of these lines to zero pressure gives the amount of adsorbed gas for total and reversible adsorption, respectively. A complete reduction of the metal surface in used pretreatment conditions and dissociative adsorption of H_2 on ruthenium were used as assumptions in calculations [28].

The metal dispersion (D) is defined as the number of metal atoms as determined on the sample surface divided by the total number of metal atoms using Eq. (1):

$$D = (V_m/22414) \times S \times M_w \times (100/X_m), \quad (1)$$

in which D is the dispersion in %, V_m is the mono-layer coverage in cm^3/g, S is the stoichiometric factor of H_2 to Ru atoms ($S = 2$), M_w the molar weight of ruthenium (101.07 g/mol) and X_m the weight fraction of metal on the catalyst [28].

The surface area and porosity measurements (physisorption) were performed with a Coulter Omnisorp 100C× gas adsorption instrument using static volumetric adsorption and desorption method. After loading the sample, the sample holder was first evacuated at room temperature to a pressure of 1.33×10^{-7} bar or lower. Then, the evacuating temperature was raised slowly to 90 °C, avoiding the pressure raise over 1.33×10^{-6} bar. At 90 °C the sample was evacuated a few hours, at least until the pressure was $1.33.10^{-7}$ bar or lower. Nitrogen was used as an adsorptive gas and the measurement was done at a temperature of liquid nitrogen bath, −196 °C. The adsorption isotherm was measured by dosing nitrogen to the sample with 0.27 bar doses and measuring the adsorbed amount as a function of the nitrogen pressure. Nitrogen pressure was increased until 98.1% of the nitrogen saturation pressure was reached. The desorption isotherms were measured by decreasing the nitrogen pressure on the sample holder gradually, with steps of 0.04 bar. The dead volume of the system was measured with helium adsorption before the measurement.

The total surface area of the sample was calculated using the Brunauer–Emmett–Teller (BET) method in the adsorption isotherm from 0.05 to 0.25 relative pressures (p/p_o, meaning absolute pressure on the sample/nitrogen saturation pressure at temperature of the measurement, liquid nitrogen bath) [29]. The pore volume and the pore size distribution of mesopores were calculated from desorption isotherm using the BJH (Barrett, Joyner and Hallender) method with a cylindrical pore model assumption [30].

Samples for Transmission Electron Microscopy (TEM) were prepared by deposition of the catalyst on a cupper grid. Bright-Field TEM images and Selected Area Electron Diffraction Patterns were recorded using a JEOL 2110F TEM operating at 200 kV. Energy Dispersive X-ray Spectrometry (EDAX) attached to the TEM was also used to determine the local chemical composition of the prepared TEM samples with a spatial resolution down to about 1 nm.

ICP was performed on a PerkinElmer 4300 DV. Solid samples were calcined at 900 °C and subsequently dissolved in a 2 wt.% HNO_3 solution. Liquid samples were only dissolved in a 2 wt.% HNO_3 solution before analysis.

2.7. Determination of the experimental error in elemental compositions and product yields

The yields and elemental compositions for each experiment were measured at least in duplicate. The relative experimental error for the elemental composition of a product obtained at a certain experimental condition was calculated by dividing the standard deviation by the average value multiplied by 100%. All relative experimental errors were averaged for the entire data set to give an average relative experimental error of 3.5% for the elemental compositions. The relative experimental error (5.7%) for the yield in case of the phenol model component experiments was obtained by calculating the relative standard deviation for the experiments at a certain condition and averaged for all experiments.

The relative experimental error (1.9%) for the methane concentration was obtained by calculating the relative standard deviation for experiments at a certain condition and averaged for all experiments.

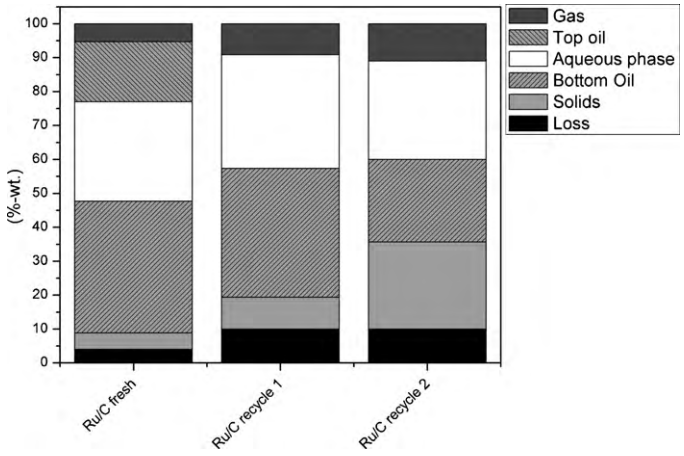

Fig. 1. Mass balance closure for the hydrotreatment experiments with fresh and reused Ru/C catalyst (350 °C, 200 bar, 4.3 h).

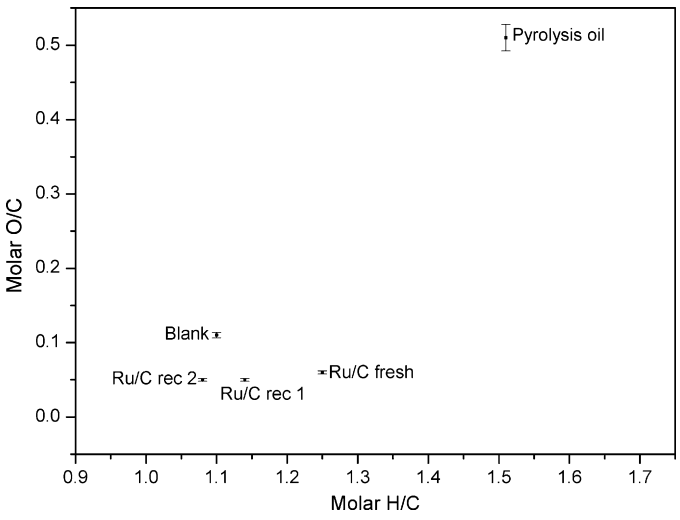

Fig. 2. The Van Krevelen plot (dry base) for the oil phase obtained after hydrotreatment of pyrolysis oil with fresh and recycled Ru/C catalyst (350 °C, 200 bar, 4.3 h). In the case of fresh Ru/C, two oil phases were obtained and the weight average composition is shown.

3. Results and discussion

3.1. Experimental studies on the hydrotreatment of fast pyrolysis oil using a commercial Ru/C catalyst

To gain insight in the stability of Ru/C catalysts in the hydrotreatment of fast pyrolysis oil, three successive experiments were carried out in a batch reactor set-up at constant pressure (hydrogen supply). In the first experiment, the autoclave was charged with a commercial sample of Ru/C and fast pyrolysis oil. The hydrotreatment reaction was carried out at 350 °C at a constant pressure of 200 bar for 4.3 h. After reaction, the products were separated from the catalyst and the catalyst was reused in a second experiment with fresh pyrolysis oil. This sequence was repeated again, giving in total three different upgraded pyrolysis oils.

After reaction, the gas, liquid and solid phase were isolated and quantified, allowing construction of the mass balance. Mass balance closure was good and ranged between 90 and 96 wt.%. The results are given in Fig. 1. The use of fresh Ru/C resulted in a liquid product consisting of three layers, *viz*. a dark brown product floating on top ('top oil'), an orange/red aqueous phase, and a dark brown layer heavier than water ('bottom layer'). In addition, gaseous and solid products were formed. For both experiments using the recycled catalyst, the liquid phase after reaction consisted only of two layers, a dark brown bottom layer with a density higher than water and an aqueous phase. The total amount of oily product(s) decreased with the number of recycles (55–30 wt.%), whereas the amount of gas phase (5–11 wt.%) and solids (3–20 wt.%) increased with the number of recycles. Catalyst recycling thus results in a considerable decrease in the top layer oil fraction and implies that catalyst performance is a function of the number of recycles. The formation of solids is expected to have a profound influence on the catalyst properties and may lead to pore blockage and a reduction of the internal catalyst surface area (*vide infra*).

The elemental composition of the organic liquid phase(s) after reaction was determined and the results are visualised in Fig. 2. Studies aimed to determine the molecular composition of the hydrotreated product after a hydrotreatment with Ru/C have been reported earlier. Typical reaction products in the organic phase(s) are hydrocarbons, substituted phenolics, esters and residual organic acids [7,11,17,24,31]. For fresh Ru/C, two organic phases were produced and the weight average composition is given in Fig. 2. The O/C ratio and the H/C for the top oil are 0.12 and 1.53, respectively, for the bottom oil these values are 0.01 and 0.88. Thus, the bottom oil contains far less oxygen than the top oil, and is more aromatic in character. These findings are in line with earlier research [24]. Details on differences in molecular composition in both organic phases are also given in this reference.

In addition, the elemental composition of the organic product from an experiment in the absence of catalysts but otherwise similar conditions is shown. In this case, a highly viscous, nearly solid product was obtained.

The level of deoxygenation (as expressed by the O/C ratio), appears higher for all catalytic experiments than for the non-catalytic one with hydrogen. Catalytic hydrodeoxygenation thus takes place to some extent, and oxygen levels of about 5 wt.% are achieved at the conditions applied in this study. A clear trend between the O/C ratio and the number of catalyst recycles is absent and all O/C ratios are within a rather narrow range (0.05–0.06). Thus, deoxygenation activity appears almost independent on the number of catalyst recycles.

The H/C ratio is a clear function of the number of catalyst recycles. The H/C ratio drops after subsequent recycles and after two recycles, the H/C ratio is close to that of the non-catalytic experiment. The H/C ratio is a measure for the hydrogenation activity, higher H/C ratios correspond with higher catalyst activity. The recycling experiments imply that the hydrogenation activity of the catalyst is reduced after catalyst recycling.

Of interest is the composition of the gas phase as a function of the number of catalyst recycles (Fig. 3).

The gas phase contains unreacted hydrogen but also considerable amounts of methane, CO and CO_2, in line with earlier results [24,25]. The presence of unreacted hydrogen indicates that the reactions were not carried out under hydrogen starvation conditions. The gas phase of the non-catalytic reaction (350 °C, 200 bar, 4.3 h) contained about 22 mol% of CO_2, indicating that CO_2 formation during catalytic hydrotreatment is not necessarily a catalytic pathway but may also be formed by thermal reactions. However, whereas for fresh catalyst, methane formation is significant, this is considerably lower for the recycled catalysts. This is again an indication that the catalyst structure changes upon the hydrotreatment reaction. These structural changes are probably the result of deactivation due to sintering and coke formation on the catalyst leading to a decrease in dispersion and surface area (*vide infra*).

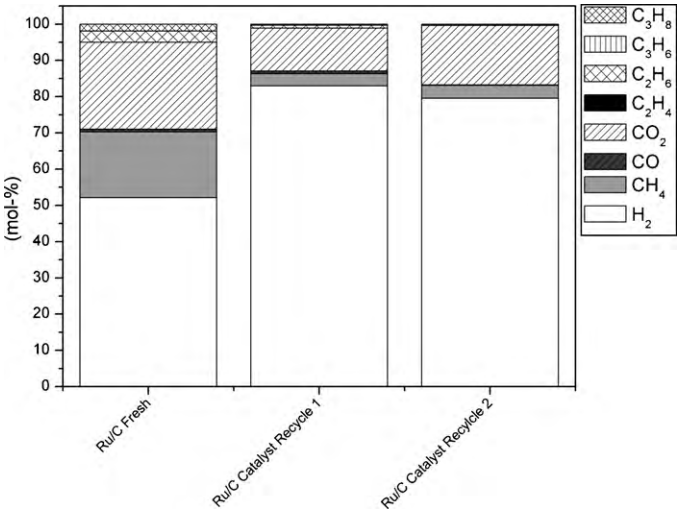

Fig. 3. Gas phase composition of the hydrotreatment experiments with fresh and reused Ru/C catalyst (350 °C, 200 bar, 4.3 h).

3.2. Hydrotreatment experiments with Ru/C prepared with different Ru-precursors and loadings

To determine the effect of the Ru-precursor on both the stability and activity of the resulting Ru/C catalysts for the hydrotreatment of fast pyrolysis oil, nine different Ru/C catalysts were synthesized by a wet impregnation method. Three different ruthenium precursors $RuCl_3$, $Ru(acac)_3$ and $Ru(NO)(NO_3)_3$ were used at three different ruthenium loadings (1, 3 and 5 wt.%). Activated carbon was used as the support for all catalysts. Catalyst performance was evaluated not only for the fast pyrolysis oil hydrotreatment but also for phenol as a model component. The commercial Ru/C catalyst sample is used as a bench mark.

3.2.1. Hydrotreatment experiments using phenol

Phenol was used as a model compound to compare the catalysts performance of the various Ru/C catalysts. The catalysts were tested at 250 °C and 100 bar of hydrogen pressure in dodecane for a reaction time of 4.3 h. Phenol was selected not only because it is known to be present in pyrolysis oil in quantities from 0.1 to 3.8 wt.% but also because the products derived thereof (cyclohexanol and cyclohexane, see Fig. 4) are easily quantified by standard analytical techniques [3]. A typical reaction profile is given in Fig. 4. Cyclohexanone, a possible intermediate, was not observed in the course of the reaction [32,33].

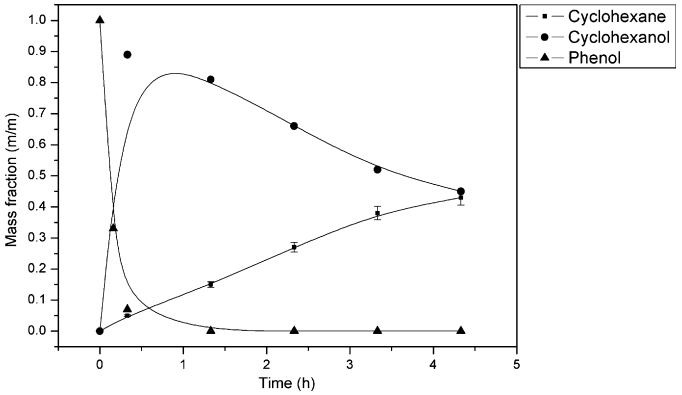

Fig. 4. Typical concentration profile for the HDO of phenol using a 5 wt.% Ru/C catalyst (250 °C, 100 bar, 4.3 h).

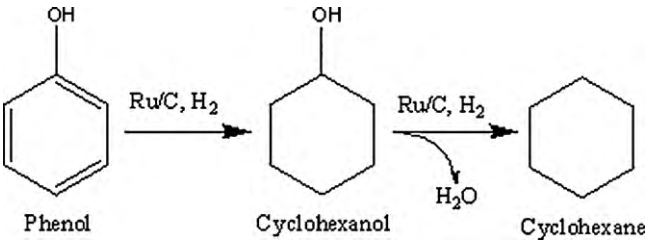

Scheme 1. Proposed reaction pathway for the hydrotreatment of phenol.

A reaction network with two reactions in series (Scheme 1) seems appropriate to explain the experimental profiles.

In all experiments the liquid phase mass balance closure was good and ranged from 88 to 100%. For all catalysts tested, the composition of the liquid phase after reaction is given in Fig. 5.

Surprisingly, the product distribution is a strong function of the ruthenium precursor used in the preparation. The best hydrogenation results (highest amounts of cyclohexane) were obtained by the commercial catalyst followed by the in-house made catalysts from the $RuCl_3$ and $Ru(acac)_3$ precursors. The catalysts prepared with the $Ru(NO)(NO_3)_3$ precursor performed considerably worse. Possible explanations are the presence of residual nitrogen on the catalyst that may have a negative effect on performance as well as a poor Ru distribution within the catalyst particle. Similar results were reported for Pd/C prepared with a nitrate precursor ($Pd(NO_3)_2$) [32]. XPS studies indicated that most Pd was deposited on the exterior of the carbon, leading to a lower overall hydrogenation activity.

The performance of the Ru/C ex-$RuCl_3$ outperforms both the catalysts based on the $Ru(NO)(NO_3)_3$ and $Ru(acac)_3$ precursors. Explanation for this good performance may be the presence of residual Cl^- in the samples, which is known to have positive effects on catalyst activity (*vide infra*) [27,34–36].

3.2.2. Hydrotreatment of pyrolysis oil using various Ru/C catalysts

All in-house prepared Ru/C catalysts were tested for the hydrotreatment of fast pyrolysis oil at 350 °C and 200 bar for a reaction time of 4.3 h with a commercial Ru/C catalyst as a reference. The visual appearance of the liquid phase after reaction is a strong function of the catalyst used in the experiments. For Ru/C catalysts with a 1 wt.% Ru loading, a highly viscous tar-like product was obtained. A similar observation was made for all catalysts prepared with $Ru(NO)(NO_3)_3$. For the 3 wt.% Ru/C catalysts prepared with $Ru(acac)_3$ and $RuCl_3$, the liquid phase consisted of two ($Ru(acac)_3$) or three ($RuCl_3$) easily flowable liquid layers. For all 5 wt.% cata-

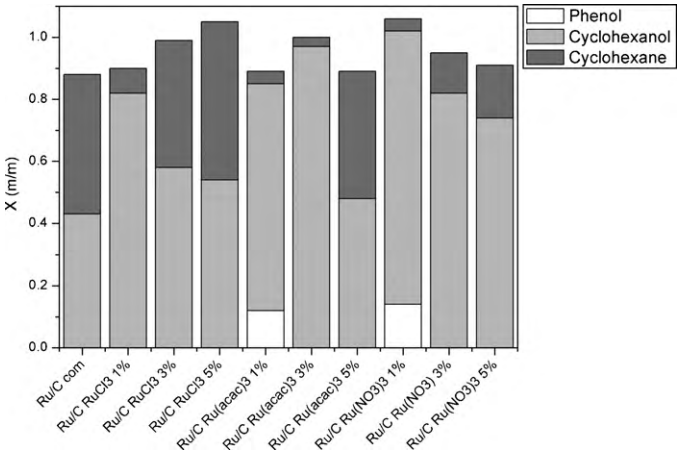

Fig. 5. Product composition of the HDO of phenol (250 °C, 100 bar) using several catalysts after 4.3 h of reaction time.

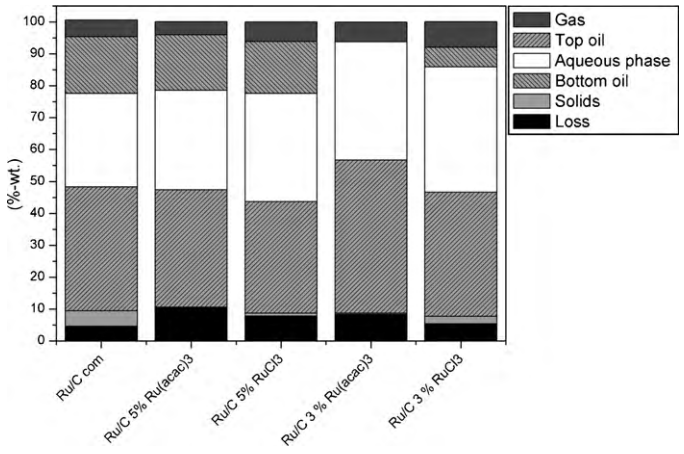

Fig. 6. Mass balances for the hydrotreatment of fast pyrolysis oil (350 °C, 200 bar, 4.3 h) using various in-house prepared Ru/C catalysts (3 and 5% loading) and a commercial Ru/C as reference.

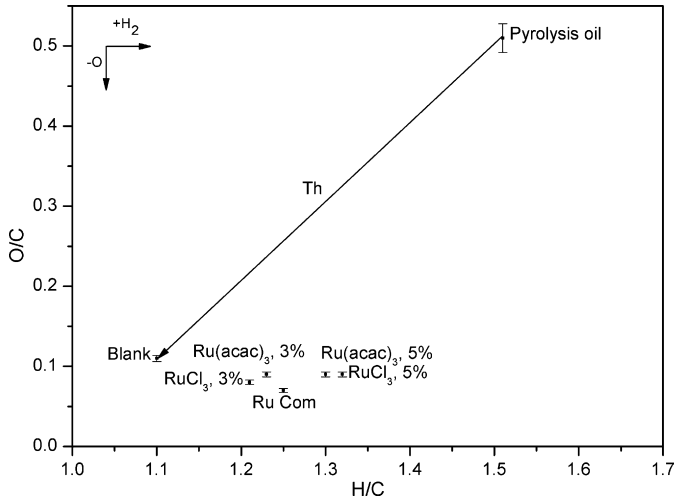

Fig. 7. The Van Krevelen plot for the oils (dry base and weight averaged elemental composition in case of two organic product phases) produced with various Ru/C catalysts (350 °C, 100 bar, 4.3 h). Th = thermal pathway.

lysts, three liquid layers were formed, a dark brown bottom layer, an intermediate aqueous phase and a brown top organic phase.

Thus, there is a strong relation between the visual appearance of the liquid phase after reaction and the activity of the catalyst as determined for the phenol hydrotreatment experiments. Poor hydrogenation catalysts will result in the formation of tar-like products, indicating polymerisation of reactive components in the mixture rather than hydrogenation activity. A similar observation was also made when performing an experiment in the absence of catalyst (*vide supra*). Intermediately active catalysts lead to the formation of two liquid phases whereas the most active catalysts produce a liquid phase consisting of three layers. The presence of a third liquid phase thus seems indicative for enhanced catalytic activity.

Due to its high viscosity, the isolation, characterization and gravimetric determination of the tar-like product from the 1 wt.% catalysts and the ones prepared with $Ru(NO)(NO_3)_3$ are troublesome. Therefore, the mass balances were only constructed for the more active catalysts leading to separate liquid phases. The results are given in Fig. 6. Mass balance closure is good for these runs (90–96 wt.%).

The total product liquid oil yield (wet basis) varied from 45 to 56 wt.%, though was essentially similar for all 5 wt.% catalysts tested. It is tempting to take the total oil yield as a measure of catalyst hydrogenation activity, with high oil yield associated with high activity. However, this is not possible as earlier studies showed that the oil yield displays an optimum with respect to the reaction time. At longer reaction times, the oil yield reduces, probably due to further conversion of the oil to gas phase components [25]. Thus, the most active catalysts do not necessarily result in the highest oil yield.

The elemental composition of the oil phases was determined and the final oxygen content of the oils ranged from 5 to 11 wt.% (Fig. 7).

The elemental composition of the product obtained in the absence of a catalyst (blank, 350 °C, 200 bar, 4 h) is also given as a measure of the thermal, non-catalytic pathway [37,38]. For the product to be of interest as a transportation fuel, the O/C ratio should preferably be lower than 0.02 and the H/C ratio should be between 1.8 and 2.0 [39]. These targets are not yet met under the process conditions applied in this study.

The Van Krevelen plot can be used to rank the catalyst with respect to activity: highly active catalysts give organic products with a low O/C ratio and high H/C ratio. For all catalysts, the O/C ratio lies within a very narrow range (0.07–0.09) and does not allow a clear discrimination in catalyst performance. A better measure seems the H/C ratio, for which the deviation between the precursors is clearly noticeable. For catalysts loaded with 5 wt.% Ru, the performance of precursors $RuCl_3$ and $Ru(acac)_3$ is slightly better than the commercial Ru catalysts. The performance of the catalysts loaded with 3 wt.% Ru is lower than the 5 wt.% catalysts.

The catalyst activity trend for the hydrotreatment of fast pyrolysis oil is essentially similar to that of the hydrotreatment of phenol (Fig. 5). Model studies with phenol thus allow selection of the preferred catalysts for actual catalytic hydrogenation of fast pyrolysis oil.

The composition of the gas phase after reaction was also determined (Fig. 8).

Besides the presence of un-reacted hydrogen, hydrocarbons (methane, ethane, ethene and higher derivatives), CO and CO_2 were present as well. The formation of methane and CO_2 occurs via two separate pathways. CO/CO_2 are formed mainly via a thermal pathway [37,38] and are known to occur on a time scale of minutes when heating up the pyrolysis oil in the absence of catalyst. In the presence of a catalyst, the catalytic route competes with the thermal route and CO_2/CO formation may be reduced by catalytic conver-

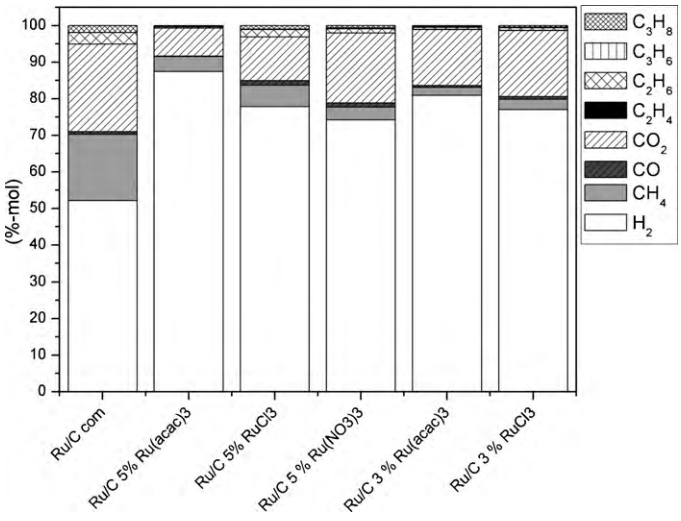

Fig. 8. Composition of the gas phase of fast pyrolysis hydrotreatment experiments (350 °C, 200 bar, 4.3 h) using various catalysts.

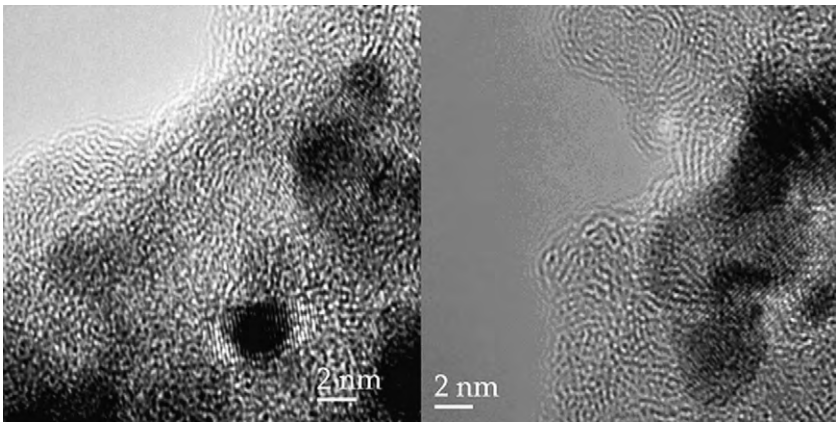

Fig. 9. TEM image of the commercial Ru/C catalyst (Left), fresh catalyst and (right) used catalyst after a HDO reaction of pyrolysis oil at 350 °C and 200 bar.

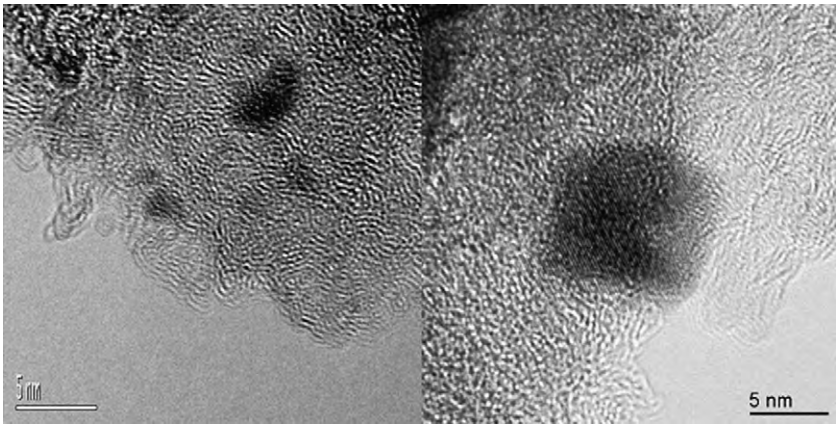

Fig. 10. TEM pictures of ex-$RuCl_3$ Ru/C before (left) and after the HDO of pyrolysis oil at 350 °C and 200 bar (right).

sions of their precursors. Thus the amount of CO_2/CO formation may differ for the various experiments with the various catalysts.

Methanation activity is typical for Ru/C catalysts [11,37], and was also observed for the catalyst recycle experiments (*vide supra*). The amount of methane is a strong function of the catalyst, with commercial Ru catalyst showing the highest methane formation. The amount of methane formed is likely related to the level of Ru dispersion on the support [40]. Metal dispersion determinations and its relation to methanation are discussed in the next paragraph.

3.3. Catalyst characterization

Recycle experiments using commercial Ru/C catalysts clearly showed that the H/C ratio of the product oil is a function on the number of recycles. The (hydrogenation) activity of the catalyst is lower after recycling, an indication for catalyst deactivation during the hydrotreatment reaction. Furthermore, distinct differences were observed between the Ru/C prepared with different precursors. The structural differences of the catalyst before and after reaction and between the catalysts prepared with different precursors were characterized using a variety of techniques such as ICP, TEM analysis, physisorption and chemisorption.

3.3.1. ICP analysis of the catalysts

A possible catalyst deactivation mechanism is loss of Ru by leaching, which might be occurring at the rather extreme operating conditions (acidity, water, temperatures of 350 °C). To gain insights in the extent of leaching, experiments were performed with the commercial Ru/C catalyst at extended reaction times (8 h) and otherwise similar conditions (350 °C and 200 bar). The Ru content of

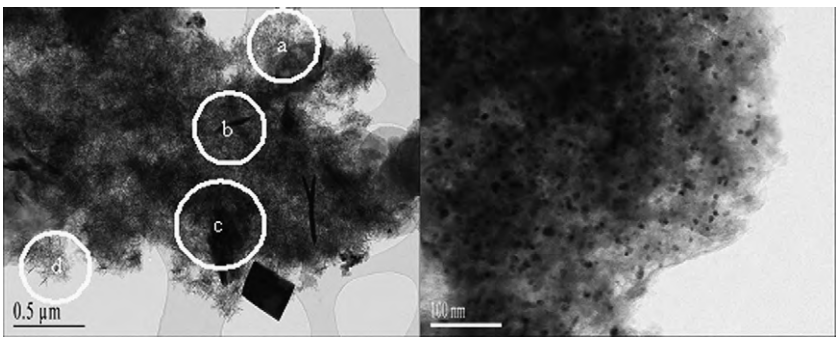

Fig. 11. TEM pictures of Ru/C prepared using $RuCl_3$ after HDO of pyrolysis oil at 350 °C and 200 bar. Left is an overview picture with a magnification of region (a), right.

Table 2
H_2 chemisorption data for the 5 wt.% Ru/C catalysts.

Sample	Total chemisorption (cm^3/g)	Total chemisorption (cm^3/g)	D (%)	D (%)
	Fresh	Used[a]	Fresh	Used[a]
Ru/C commercial	1.37	0.11	22.7	0.20
Ru/C $Ru(acac)_3$	0.39	0.13	5.90	0.30
Ru/C $RuCl_3$	0.65	0.24	9.60	2.20
Carrier	0.12	n.a.	2.10	n.a.

[a] HDO of pyrolysis oil at 350 °C and 200 bar for a reaction time of 4.3 h.

the catalyst was determined before and after reaction, and no significant differences were observed. Remarkable is the presence of large amounts of iron on the catalyst after reaction (0.87 wt.%), which is an order of magnitude higher than the fresh catalyst. The most likely source for Fe is the reactor wall and the impellor. The effect of Fe on catalytic activity and possible deactivation pathways is not yet known.

3.3.2. Characterization of Ru/C catalysts by TEM

TEM analysis was performed on two catalysts: the commercial Ru/C catalyst as a reference and the 5 wt.% catalyst prepared using $RuCl_3$. The latter catalyst was selected as it showed the highest hydrogenation activity (Fig. 7). Both catalysts were analyzed before and after the hydrotreatment reaction of fast pyrolysis oil.

Fig. 9 shows representative TEM images for the commercial Ru/C catalyst. The size of the Ru particles for the fresh catalyst is in the range of 2–5 nm, while after the reaction the size is in the range of 5–10 nm. This concerns a qualitative observation and needs support by other analysis as will be discussed in the subsequent sections.

Fig. 10 shows representative TEM pictures of the ex-$RuCl_3$-based catalyst. The fresh catalyst contains ruthenium clusters in the size range of 1–5 nm (the minimum detection range of the TEM). After reaction, the ruthenium clusters are considerably larger and up to 7 nm. Thus, for both catalysts sintering of Ru particles takes place to a great extent during the hydrotreatment reaction and this likely negatively affects catalyst activity.

Fig. 11 shows the TEM pictures under lower magnifications of the ex-$RuCl_3$ catalyst. It shows an overview with different regions highlighted (left-side, a–d) and a magnification of section (a, right-side).

In Fig. 11 four types of patterns can be distinguished, indicated by (a–d). Section (a) shows a proper dispersion of the Ru on the catalyst surface (see also magnification in Fig. 12, right-side). Patterns (b) and (c) appear large carbon deposits with different morphology. Finally, region (d) shows crystals consisting most likely of carbon [41,42] and Ru particles that are relatively narrow in terms of cluster size.

Based on these observations, it can be concluded that the average ruthenium particle size increases during reaction and that significant amounts of coke are deposited on the catalyst surface.

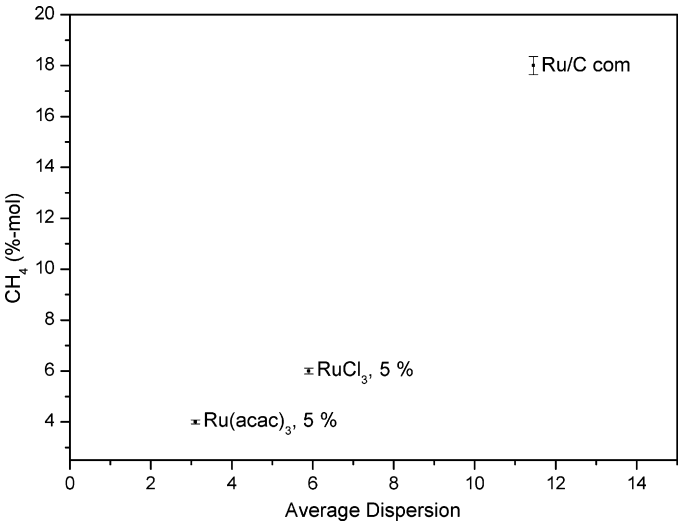

Fig. 12. Methane formation as a function of the average dispersion for the HDO of pyrolysis oil using 5 wt.% catalysts prepared with different precursors (350 °C, 200 bar, 4 h).

This concerns a very qualitative observation of a relative small part of the catalyst surface, and additional characterization techniques have been applied to support these findings (physisorption and chemisorption, see below).

3.3.3. Chemi- and physisorption data for the Ru/C catalysts

Table 2 shows the chemisorption results for a number of selected catalyst samples. The fresh commercial catalyst displays the highest dispersion (22.7%) followed by the ex-$RuCl_3$ catalyst (9.6%) and the catalyst prepared using $Ru(acac)_3$ (5.9%). After reaction, a large decrease in the dispersion was observed in all cases, with a reduction of nearly 100% (commercial catalyst), 77% (ex-$RuCl_3$) and 95% (ex-$Ru(acac)_3$).

The chemisorption data are in agreement with the TEM data and are indicative for metal sintering and coke deposition.

Gas physisorption analyses using nitrogen were carried out to determine the degree of textural changes during the reaction. Table 3 shows the results for the commercial and in-house synthesized catalysts, fresh and after reaction. The commercial catalyst

Table 3
N_2 physisorption data for the Ru/C catalysts.

	BET surface area (m^2/g)	BET surface area (m^2/g)	Total pore volume > 10 Å (cm^3/g)	Total pore volume > 10 Å (cm^3/g)
	Fresh	Used[a]	Fresh	Used[a]
Ru/C commercial	717	111	0.36	0.17
Ru/C $Ru(acac)_3$	774	169	0.41	0.26
Ru/C $RuCl_3$	794	164	0.41	0.29
Carrier	751	n.a.	0.41	n.a.

[a] After catalytic hydrotreatment reaction with pyrolysis oil at 350 °C and 200 bar for a reaction time of 4.3 h.

shows a reduction of ca. 85% in the BET surface area, compared to 78% for the catalyst ex-Ru(acac)$_3$ and 79% for the $RuCl_3$-derived catalyst.

With the chemo-and physisorption data available, the observation that catalyst performance was a function of the number of catalyst recycles (Figs. 1–3) may be rationalised. Both the oil yield and the H/C ratio were reduced considerably after recycling. These observations may be ascribed to coke formation as suggested by the BET data and sintering of Ru particles to larger aggregates (physisorption and TEM data). An additional deactivation pathway is Ru/C poisoning by metal and/or sulphur in the pyrolysis oil feed. Further investigation with a range of different pyrolysis oil feedstocks with a range of levels of metals and sulphur will be required to gain insights in this pathway and to draw conclusions.

There appears to be a relation between methane formation for the various catalysts with a 5 wt% loading and the average catalyst dispersion (Fig. 12). Apparently, a higher dispersion leads to a larger amount of methane in the gas phase. This observation is in line with data from Takenaka [40], where higher methanation rates were observed for Ru catalysts with high dispersions. However, recent publications indicate that methanation activity is very structure sensitive and is among others a function of support and reaction conditions [43,44]. Thus, the observed reduction in methane formation for the recycling experiments (Fig. 1) is likely related to a reduction of the metal dispersion.

4. Conclusions

Catalyst recycling experiments in a batch reactor set-up indicate that the performance of Ru/C during the catalytic hydrotreatment of fast pyrolysis oil is a function of the number of recycles. The oil yield (55–30 wt.%) and the H/C ratio (1.24 for fresh Ru/C to 1.08 for twice recycled Ru/C) of the product oils are reduced considerably after subsequent catalyst recycles. After two recycles, the H/C ratio is even close to that of the blank experiment without catalyst, indicating severe loss in hydrogenation activity upon recycling. Analyses of the catalyst before and after reaction by TEM, physi- and chemisorption techniques indicate that clustering of metal particles and coke deposition occurs to a significant extent. Further testing in dedicated continuous units at extended reaction times is required to gain detailed insights in long-term catalyst stability.

Furthermore, nine different catalysts have been synthesized using different precursors and different loading namely 1, 3 and 5 wt.% to determine the effect of the type of catalyst precursor on catalyst performance for the hydrotreatment of fast pyrolysis oil (350 °C, 200 bar for 4.3 h) and phenol. The best results with respect to the hydrogenation activity as expressed by the H/C ratio of the product (1.32) were observed for the catalyst prepared with 5 wt.% $RuCl_3$. This catalyst showed the lowest decrease in BET area and dispersion after reaction. These findings may be applied to develop improved Ru/C catalysts for the hydrotreatment of fast pyrolysis oil.

Acknowledgements

Hans van der Velde (University of Groningen, Department of Organic Chemistry) is acknowledged for performing the elemental analysis. Andrea Gutierrez (Helsinki University of Technology, Department of Chemical Technology) is acknowledged for performing chemi- and physisorption experiments. Prof. dr. ir. B.J. Kooi (University of Groningen, department of Applied Physics, Zernike Institute for Advanced Materials) is acknowledged for performing and assistance with interpretation of the TEM-EDAX analysis. This project was financially supported by Senter Novem (projects NEO 0268-02-03-03-0001 and DEN 2020-04-90-08-001)

References

[1] G.W. Huber, A. Corma, Chem. Rev. 106 (2006) 4044–4098.
[2] A. Bridgwater, S. Czernik, J. Diebold, D. Meier, A. Oasmaa, C. Peacocke, Fast Pyrolysis of Biomass: a Handbook, vol. 1, CPL Press, Berkshire, 1999.
[3] J.P.A. Diebold, Review of the Chemical and Physical Mechanisms of the Storage Stability of Fast Pyrolysis Bio-Oils, NREL/SR-570-27613, Colerado, USA, 2000.
[4] D.C. Elliott, E.G. Baker, Biotechnol. Bioeng. Symp. Suppl. 14 (1984) 159–174.
[5] J. Gagnon, S. Kaliaguine, Ind. Eng. Chem. Res. 27 (1988) 1783–1788.
[6] A. Oasmaa, D.G.B. Boocock, Can. J. Chem. Eng. 70 (1992) 294–300.
[7] F. Mahfud, Exploratory Studies on Fast Pyrolysis Oil Upgrading, PhD Thesis, University of Groningen, The Netherlands, 2007.
[8] S.P. Zhang, Energ. Source 25 (2003) 57–65.
[9] E. Furimsky, F.E. Massoth, Catal. Today 52 (1999) 381–495.
[10] W. Baldauf, U. Balfanz, M. Rupp, Biomass Bioeng. 7 (1994) 237–244.
[11] D.C. Elliott, Energy Fuels 21 (3) (2007) 1792–1815.
[12] S.B. Gevert, M. Eriksson, P. Eriksson, F.E. Massoth, Appl. Catal. A 117 (2) (1994) 151–162.
[13] J.E. Otterstedt, S.B. Gevert, S.G. Jaras, P.G. Menon, Appl. Catal. 22 (2) (1986) 159–179.
[14] W.G. Appleby, G.M. Good, J.W. Gibson, Ind. Eng. Chem. Proc. Des. Dev. 1 (2) (1962) 102–110.
[15] E. Laurent, B. Delmon, Appl. Catal. A 109 (1) (1994) 77–96.
[16] A. Centeno, E. Laurent, B. Delmon, J. Catal. 154 (2) (1995) 288–298.
[17] J. Wildschut, J. Arentz, C.B. Rasrendra, R.H. Venderbosch, H.J. Heeres, Environ. Prog. Sust. Energ. 23 (8) (2009) 450–460.
[18] L. Conti, G. Scano, J. Boufala, S. Mascia, in: A.V. Bridgwater, E.N. Hogan (Eds.), Bio-Oil Production and Utilization, CPL Press, Newbury Berks, 1996, pp. 198–205.
[19] D.C. Elliott, G.F. Schiefelbein, Abstr. Pap. Am. Chem. Soc. 34 (1989) 1160–1166.
[20] D.C. Elliott, G.G. Neuenschwander, in: A.V. Bridgwater, D.G.B. Boocock (Eds.), Developments in Thermochemical Biomass Conversion, vol. 1, Blackie Academic & Professional, London, 1996, pp. 611–621.
[21] D.C. Elliott, K.L. Peterson, D.S. Muzatko, E.V. Alderson, T.R. Hart, G.G. Neuenschwander, Appl. Biochem. Biotech. 113 (2004) 807–825.
[22] M.C. Samolada, W. Baldauf, I.A. Vasalos, Fuel 77 (1998) 1667–1675.
[23] Y.H.E. Sheu, R.G. Anthony, E.J. Soltes, Fuel Process. Technol. 19 (1988) 31–50.
[24] J. Wildschut, F.H. Mahfud, R.H. Venderbosch, H.J. Heeres, Ind. Eng. Chem. Res. 48 (23) (2009) 10324–10334.
[25] J. Wildschut, H.J. Heeres, Prepr. Pap. – Am. Chem. Soc., Div. Fuel. Chem. 53 (1) (2008) 349–350.
[26] T. Miyazawa, S. Koso, K. Kunimori, K. Tomishige, Appl. Catal. A 318 (2007) 244–251.
[27] G. Neri, L. Mercadante, A. Donato, A.M. Visco, S. Galvagno, Catal. Lett. 29 (1994) 379–386.
[28] X. Shen, L.J. Garces, Y. Ding, K. Laubernds, R.P. Zerger, M. Aindow, E.J. Neth, S.L. Suib, Appl. Catal. A 335 (2008) 187–195.
[29] S. Brunauer, P.H. Emett, E. Teller, J. Am. Chem. Soc. 60 (1938) 309–319.
[30] E.P. Barrett, L.G. Joyner, P.P. Halenda, J. Am. Chem. Soc. 73 (1951) 373–380.
[31] J.H. Marsman, J. Wildschut, F.H. Mahfud, H.J. Heeres, J. Chromatogr. A 1150 (2007) 21–27.
[32] E. Diaz, A.F. Mohedano, L. Calvo, M.A. Gilarranz, J.A. Casas, J.J. Rodriguez, Chem. Eng. J. 131 (2007) 65–71.
[33] C. Zao, Y. Kuo, A.A. Lemonidou, X. Li, J.A. Lercher, Angew. Chem. Int. Eng. Ed. 48 (22) (2009) 3987–3990.
[34] D. Jiang, Y. Ding, Z. Pan, X. Li, G. Jiao, J. Li, et al., Appl. Catal. A 331 (2007) 70–77.
[35] J.G. Kim, S.S. Kim, J. Ind. Eng. Chem. 12 (2) (2006) 284–288.
[36] M. Ojeda, M.L. Granados, S. Rojas, P. Terreros, J.L.G. Fierro, J. Mol. Catal. A: Chem. 202 (1–2) (2003) 179–186.
[37] R.H. Venderbosch, A.R. Ardiyanti, J. Wildschut, A. Oasmaa, H.J. Heeres, J. Chem. Technol. Biotechnol. 85 (2010) 674.
[38] M. Rep, R.H. Venderbosch, D. Assink, W. Tromp, S.R.A. Kersten, W. Prins, W.P.M. van Swaaij, in: A.V. Bridgwater (Ed.), Science in Thermal and Chemical Biomass Conversion, CPL Press, Newbury Berkshire, 2006, pp. 1526–1535.
[39] S.R.A. Kersten, W.P.M. van Swaaij, L. Lefferts, K. Seshan, in: G. Centi, R.A. van Santen (Eds.), Catalysis for Renewables: from Feedstock to Energy Production, Wiley-VCH, Chichester, 2007, pp. 119–141.
[40] S. Takenaka, T. Shimizu, K. Otsuka, Int. J. Hydrogen Energy 29 (2004) 1065–1073.
[41] S.H. Yu, X. Cui, L. Lingling, K. Li, B. Yu, M. Antonietti, H. Cölfen, Adv. Mat. 16 (2004) 1636–1640.
[42] B. Hu, S.H. Yu, K. Wang, L. Liu, X.W. Xu, Dalton Trans. 40 (2008) 5414–5423.
[43] M. Osada, O. Sato, K. Arai, M. Shirai, Energy Fuels 20 (2006) 2337–2343.
[44] P. Panagiotopoulou, D.I. Kondarides, X.E. Verykios, Appl. Catal. B 88 (2009) 470–478.